Supporting Information

Long-Term Electrocatalytic N_2 Fixation by MOF-Derived Y-Stabilized ZrO_2: An Insight into Deactivation Mechanism

Shijian Luo,[a] Xiaoman Li,[a,*] Mingyuan Wang,[b] Xu Zhang,[a] Wanguo Gao,[a] Senda Su,[a] Guiwu Liu,[b,*] and Min Luo[a,*]

a. State Key Laboratory of High-efficiency Utilization of Coal and Green Chemical Engineering, School of Chemistry and Chemical Engineering, Ningxia University, Yinchuan, Ningxia, 750021, China

b. School of Materials Science and Engineering, Jiangsu University, Zhenjiang, Jiangsu, 212013, China

*Corresponding author: Min Luo martinluomin@163.com,

Xiaoman Li lixm2017@nxu.edu.cn,

Guiwu Liu gwliu76@ujs.edu.cn

Content

EXPERIMENTAL SECTION

Materials

All reagents used in this experiment were of analytical grade without further purification. Zirconium chloride ($ZrCl_4$, 98%), yttrium chloride (YCl_3, 98%), terephthalic acid (H_2BDC, 99%), acetic acid ($C_2H_4O_2$, 99.5%) and N, N-dimethylformamide (DMF, 99.8%) were purchased from Aladdin chemistry Co. Acetone (99.5%) were purchased from Sinopharm Chemical Reagent Co. Nafion (5 wt%) were purchased from Sigma-Aldrich Chemical Reagent Co.,Ltd. Deionized water was purified through a Millipore system.

Synthesis of precursor UiO-66 and Y-UiO-66

First, zirconium chloride was selected as the zirconium source, yttrium chloride as the yttrium source, terephthalic acid as the ligand, and acetic acid as the conditioner. Typically, 0.507 mmol $ZrCl_4$, 0.031 mmol YCl_3 and 0.507 mmol H_2BDC and 26 ml DMF were put into a 50 mL Telfon vessel and stirred for 30 min until a homogeneous clear solution is obtained. Then 1 mL acetic acid was added. After magnetically stirred for 30 min, the above mixture was placed in autoclave and reacted at 120 ℃ for 24 hours. The precipitate was washed alternately with DMF and acetone by centrifugation. The solid product (Y-UiO-66) was collected and dried in a vacuum oven at 80 ℃ for 12 h. If YCl_3 wasn't added in the above process, the product is UiO-66.

Synthesis of C@YSZ and C@ZrO_2 electrocatalysts

Y-UiO-66 was heated in a furnace in Ar from room temperature to 900℃ at a heating rate of 2℃ min^{-1} and maintained for 2 h to obtain C@YSZ electrocatalyst. UiO-66 was heated in a furnace in Ar from room temperature to 900℃ at a heating rate of 2℃ min^{-1} and maintained for 2 h to obtain C@ZrO_2 electrocatalyst.

Synthesis of monoclinic C@ZrO_2-600 sample

UiO-66 was heated in a furnace in Ar from room temperature to 600℃ at a heating rate of 2℃ min^{-1} and maintained for 2 h to obtain monoclinic C@ZrO_2-600 sample.

Preparation of working electrode

The carbon paper was sonicated for 1 h in ethanol solution and dried at ambient condition. 10 mg catalyst and 100 μL of Nafion solution (5 wt%) were dispersed in mixed solution contain 700 μL isopropanol and 200 μL H_2O by 1 h sonication to form a homogeneous ink. Then 20 μL catalyst ink was loaded on a 1×1 cm^2 carbon paper and dried at 60℃ for 12 h.

Characterizations

X-ray diffraction (XRD) data were obtained from an AXS D8 ADVANCE A25 with Cu Kα radiation (40 kV, 40 mA) of wavelength 0.154 nm (Germany). SEM images and Energy Dispersive Spectrometer (EDS) were collected from the ZEISS EVO18 scanning electron microscope at an accelerating voltage of 40 kV (Germany). TEM images were obtained from a

FEI Talos 200S transmission electron microscope operated at 200 kV. The size of prepared samples is measured by a NanoMeasurer 1.2 software. XPS measurements were performed on a Thermo escalab 250Xi X-ray photoelectron spectrometer using Mg as the exciting source. The Raman spectra were collected on a Thermo Fisher Raman spectrometer under a backscattering geometry (λ= 532 nm). The electron paramagnetic resonance (EPR) were obtained from Bruker A300-10/12 system. Temperature programmed desorption (TPD) were carried out on an AutoChem II 2920 system. Nuclear magnetic resonance was tested on a Bruker AVANCE III 600 MHz system. The absorbance data of spectrophotometer were measured on Persee TU-19 UV-Vis spectrophotometer. The Ion chromatography (IC) were tested on an Agilent 7500ce system.

Electrochemical measurements

N_2 reduction experiments were carried out in a two-compartment cell, which was separated by the Nafion 211 membrane. The electrochemical experiments were performed with a CHI 660E electrochemical analyzer (CH Instruments, Inc., Shanghai, China) using a three-electrode configuration including prepared working electrode, platinum sheet electrode and saturated Ag/AgCl (saturated KCl electrolyte) serving as the working electrode, counter electrode and reference electrode, respectively. The potentials reported in this work were converted to RHE scale via calibration with the following equation: E (vs. RHE) = E (vs. Ag/AgCl) + 0.197 + 0.059 × pH. For N_2 reduction experiments, the 0.1 M Na_2SO_4 electrolyte was purged with N_2 for 30 min before the measurement. Potentiostatic test was conducted in N_2-saturated 0.1 M Na_2SO_4 solution (70 mL) for 1 hour. Each NRR test was repeated at least three times. The error bar was based on the standard deviation (SD) for three times NRR tests.

Determination of NH_4^+

NH_3/NH_4^+ concentration analysis was conducted using Nessler's reagent method. First, 50 mL of the solution was placed in a 50 mL flask. Then, 1 mL of the potassium sodium tartrate solution was added to the flask. After blending, 1 mL of Nessler's reagent was added to the same flask and mixed. Then, the mixture was left to stand for 10 min for full color processing. Finally, the concentration of NH_3/NH_4^+ was tested using an UV-vis spectrophotometer at 420 nm wavelength. The fitting curve ($y = 0.1685x + 0.008$, $R^2 = 0.998$) shows good linear relation of absorbance value with NH_4^+ concentration.

Determination of N_2H_4

The N_2H_4 in the electrolyte was estimated by the method of Watt and Chrisp. A mixture of $C_9H_{11}NO$ (5.99 g), HCl (concentrated, 30 mL) and ethanol (300 mL) was used as a color reagent. In detail, 5 mL electrolyte was removed from the electrochemical reaction vessel and added into 5 mL above prepared color reagent and stirring 15 min at room temperature. The absorbance of the resulting solution was measured at 455 nm. The concentration absorbance curves were calibrated using standard $N_2H_4 \cdot H_2O$ solution with a series of concentrations. The fitting curve ($y = 1.6331x + 0.0187$, $R^2 = 0.999$) shows good linear relation of absorbance value with N_2H_4

concentration.

Isotope labeling experiment and NMR test.

The $^{15}N_2$ isotopic labeling experiment was carried out using $^{15}N_2$ as the feeding gas (Shanghai Research Institute of Chemical Industry C, 98 atom % ^{15}N) with 0.1 M Na_2SO_4 electrolyte. After electrolysis at −0.5 V vs. RHE for 2 h, 10 mL of the electrolyte was taken out and acidized to pH ~3 by adding 0.5 M H_2SO_4. Afterwards, 0.9 mL of the resulting solution was taken out and mixed with 0.1 mL D_2O containing 100 ppm dimethyl-sulphoxide (Sigma-Aldrich, 99.99%) as an internal standard for ^1H nuclear magnetic resonance measurement (^1H NMR, Bruker Avance III 600 MHz).

Long-term stability test

Long-term NRR test was conducted in 0.1 M Na_2SO_4 solution (90 mL) for 7 days under N_2-saturated atmosphere and isothermal conditions. At the first hour, first day, third day, 5th day and 7th day of NRR test, 10 mL electrolyte was taken to measure the ammonia concentration through Nessler's reagent method. The long-term stability tests were repeated three times to reduce errors caused by environmental factors.

Calculations of NH_3 formation rate and Faradaic efficiency (FE)

The rate of formation of NH_3 was calculated using the following equation:

$$v_{NH_3} = \frac{[NH_3]\times V}{t\times m_{cat.}}$$

The FE was calculated according to the following equation:

$$FE = \frac{3\times F\times[NH_3]\times V}{17\times Q}$$

where $[NH_3]$ is the measured concentration of NH_4^+ ions; V is the volume of the cathodic reaction electrolyte; t is the time for which the potential was applied; m is the mass of catalyst loaded on the working electrode; F is the Faraday constant; and Q is the quantity of applied charge/electricity.

In-situ electrochemical quartz-crystal microbalance (EQCM) tests

The working electrode is prepared as follow: 10 mg catalyst and 100 μL of Nafion solution (5 wt %) were dispersed in mixed solution contain 700 μL isopropanol and 200 μL H_2O by 1 h sonication to form a homogeneous ink. Then 20 μL catalyst ink was loaded on the Quartz crystal and dried at 80℃ for 24 h. The saturated Ag/AgCl electrode and Pt electrode were served as the reference electrode and the counter electrode. The electrolyte was 0.1 M Na_2SO_4. The mass change (Δm) was calculated by following equation.

$$\Delta m = -\frac{\sqrt{\rho_q \mu_q}}{2f_0} \times \Delta f = -C_f \Delta f$$

where Δf is the varication of frequency, C_f is the sensitivity factor of a quartz crystal (1.46 ng

Hz^{1-}), ρ_q is the density of a quartz crystal (2.648 g cm^{-3}), μ_q is the shear modulus of a quartz crystal, f_0 is the fundamental frequency of a quartz crystal (8 MHz).

DFT calculation details

All calculations were performed using first-principles calculations based on DFT through the Vienna ab initio simulation package (VASP). The Perdew-Burke-Ernzerhof (PBE) exchange-correction functional for generalized gradient approximation (GGA) was used to optimize all the geometric structures and the interactions between ions and valence electrons were described by the super soft pseudopotential. The kinetic energy cutoff for the plane wave basis was set as 500 eV. A 3 × 3 × 1 Monkhorst−Pack k-point sampling was used for all the surfaces and A vacuum space of at least 20 Å was included in the unit cell. All structures were relaxed until the forces exerted on each atom were less than 0.01 eV/Å. The energy convergence criteria for electronic and ionic iterations were assumed to be 10-5 and 10-4 eV, respectively. In this article, a 2 × 2 × 4 supercell ZrO_2 (011) with one O-vacancy and a Y atom substitutes Zr atom of ZrO_2 (011) with one O-vacancy are constructed to calculate the thermodynamic stability of the surface O-vacancies. The bottom two layers were fixed to similuate the bulk, whereas the two topmost layers were allowed to fully relax. And the thermodynamic stability of O-Vacancies on the surfaces is calculated according to following formula:

$$\Delta E_{vac} = E_{vac,2} - E_{vac,1}$$

Where $E_{vac,2}$ represent the energy of an O-vacancy in the first subsurface layer; $E_{vac,1}$ represent the energy of ZrO_2 slab with an O-vacancy in the surface layer.

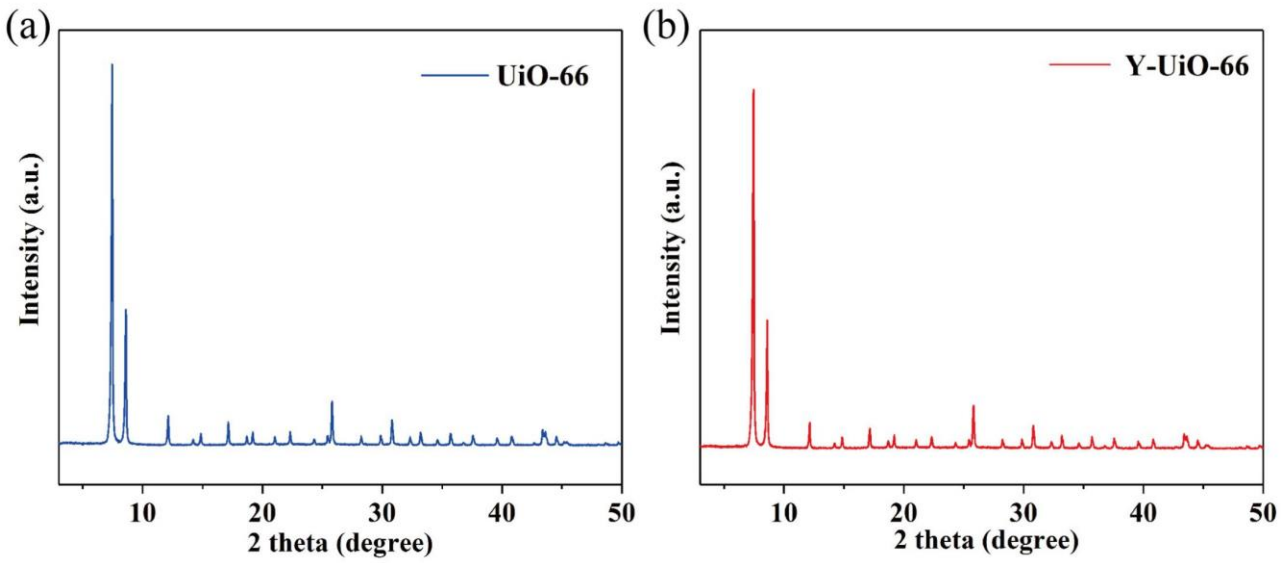

Fig. S1. (a) XRD pattern of UiO-66. (b) XRD pattern of Y-UiO-66.

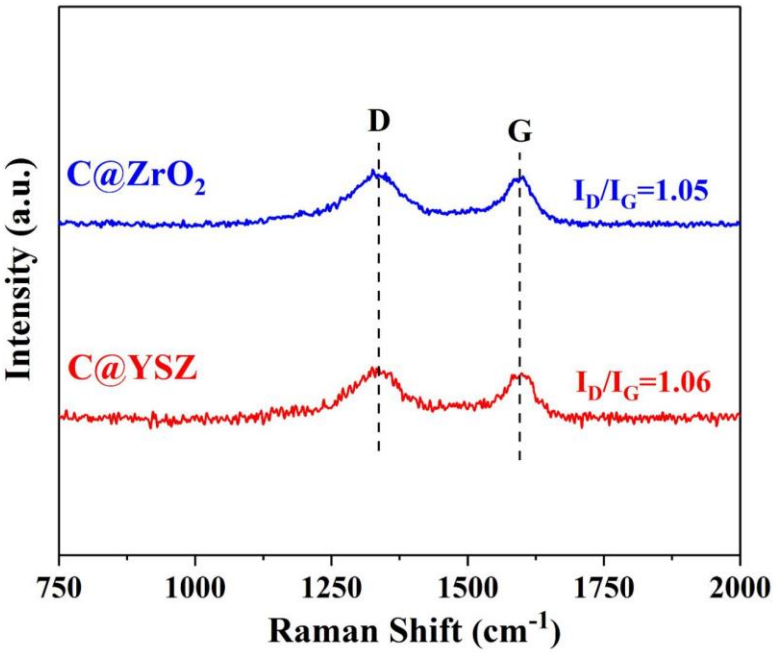

Fig. S2. The Raman pattern of C@YSZ and C@ZrO_2.

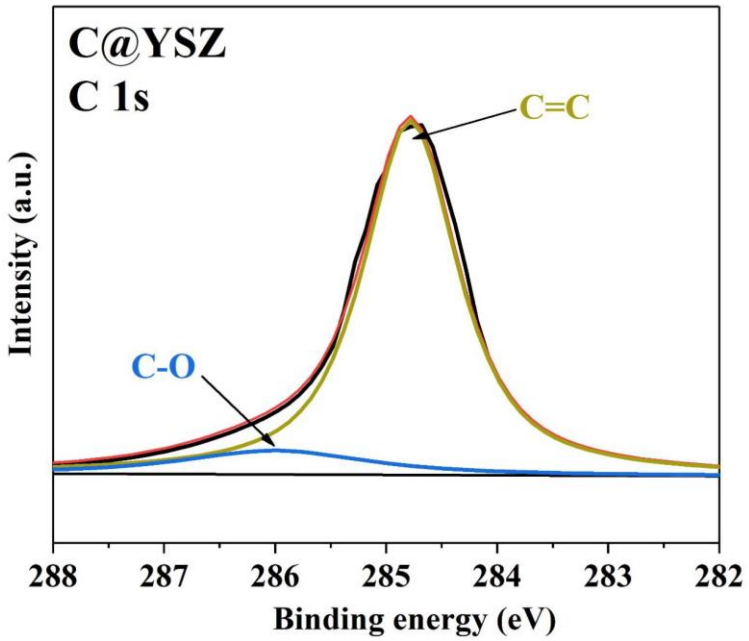

Fig. S3. XPS C 1s spectra for the C@YSZ.

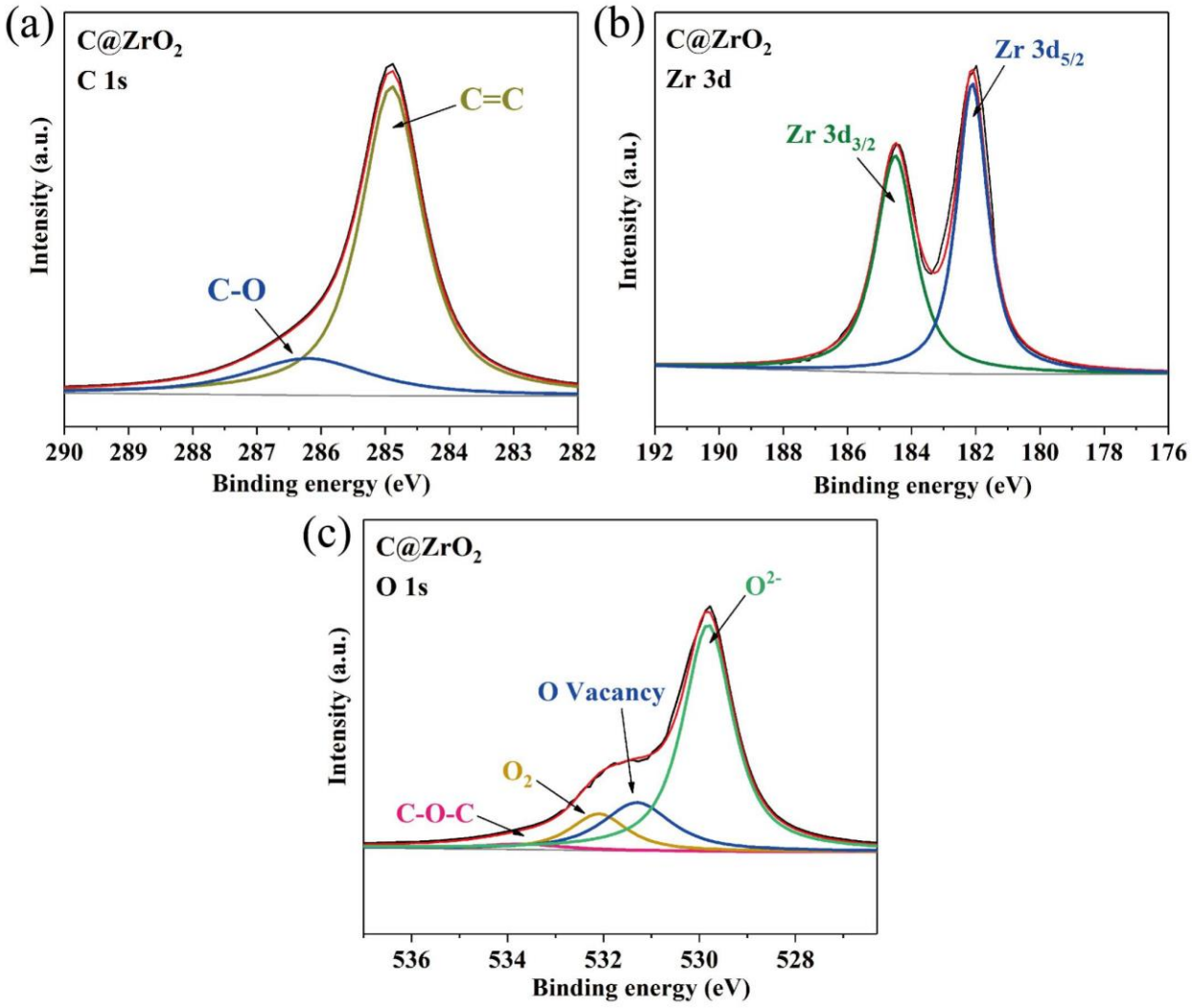

Fig. S4. (a) XPS C 1s spectra, (b) XPS Zr 3d spectra and (c) XPS O 1s spectra of the C@ZrO_2.

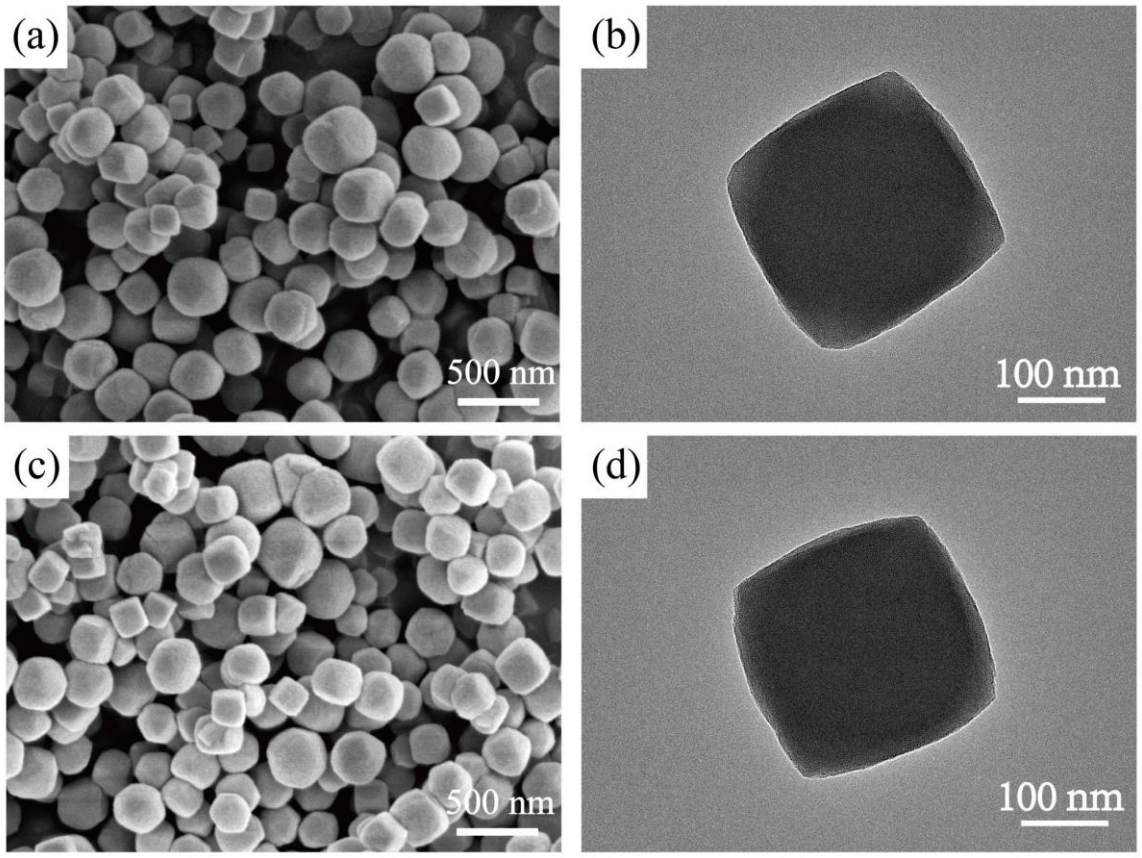

Fig. S5. SEM and TEM image of UiO-66 (a), (b) and Y-UiO-66 (c), (d).

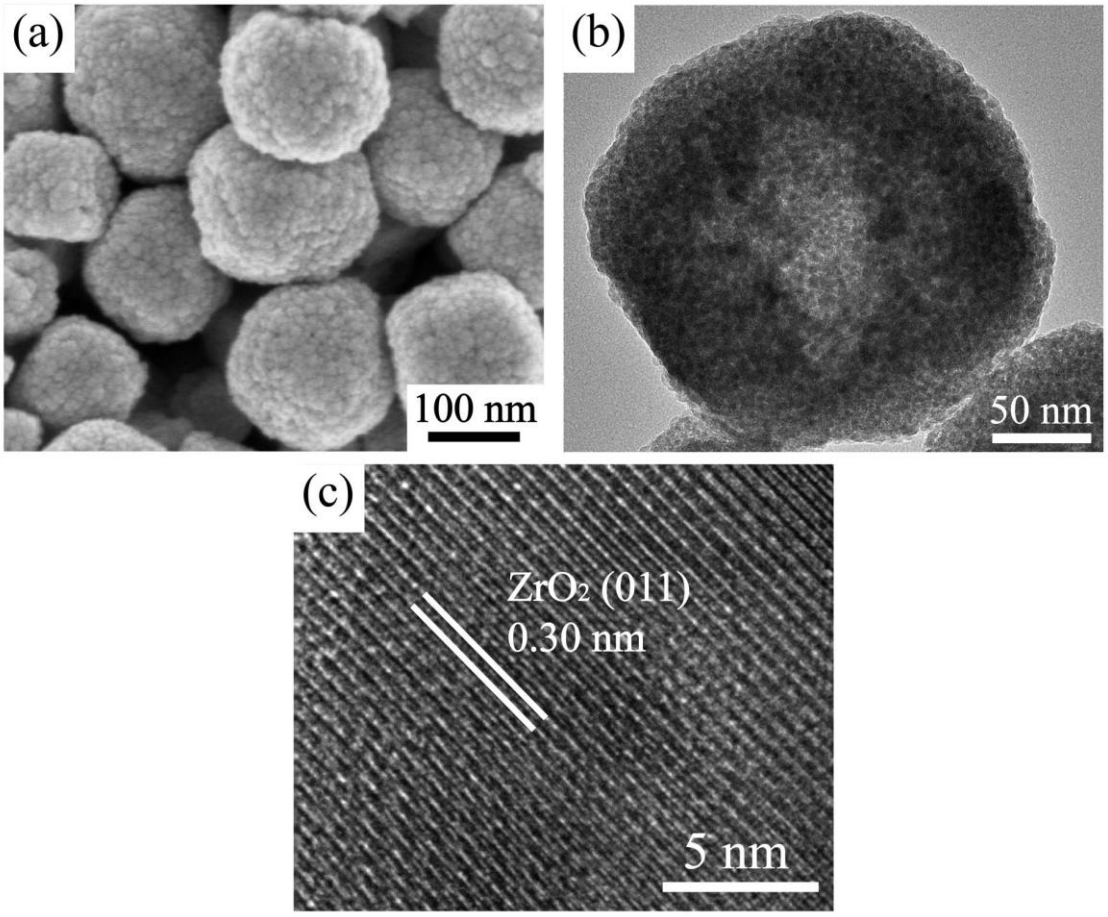

Fig. S6. (a) SEM image, (b) TEM image and (c) HRTEM image of C@ZrO_2.

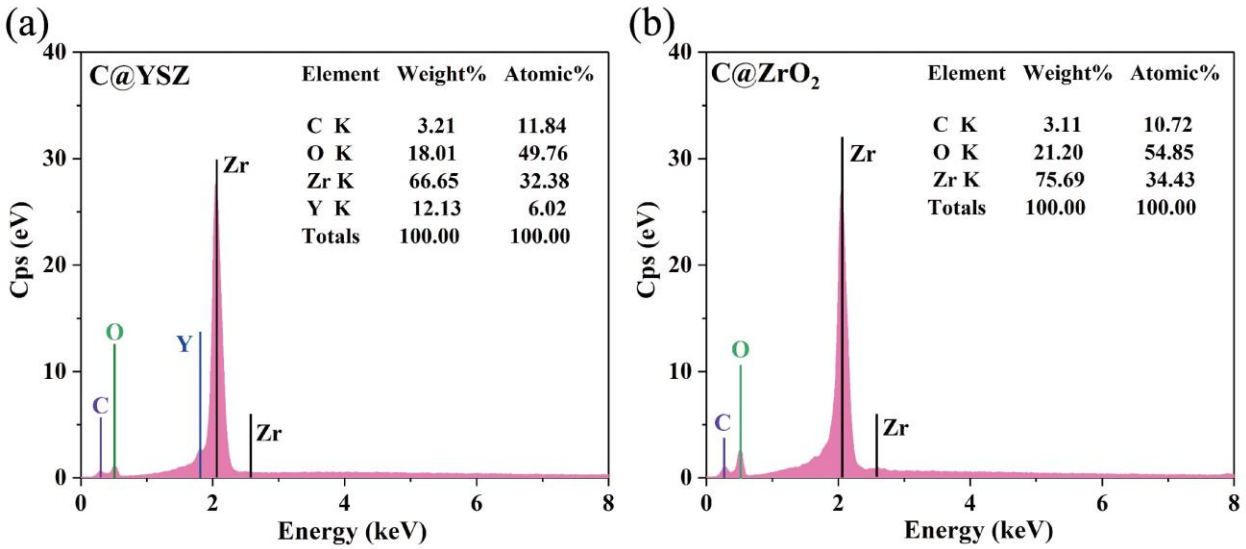

Fig. S7. (a) EDX data of C@YSZ. (b) EDX data of C@ZrO_2.

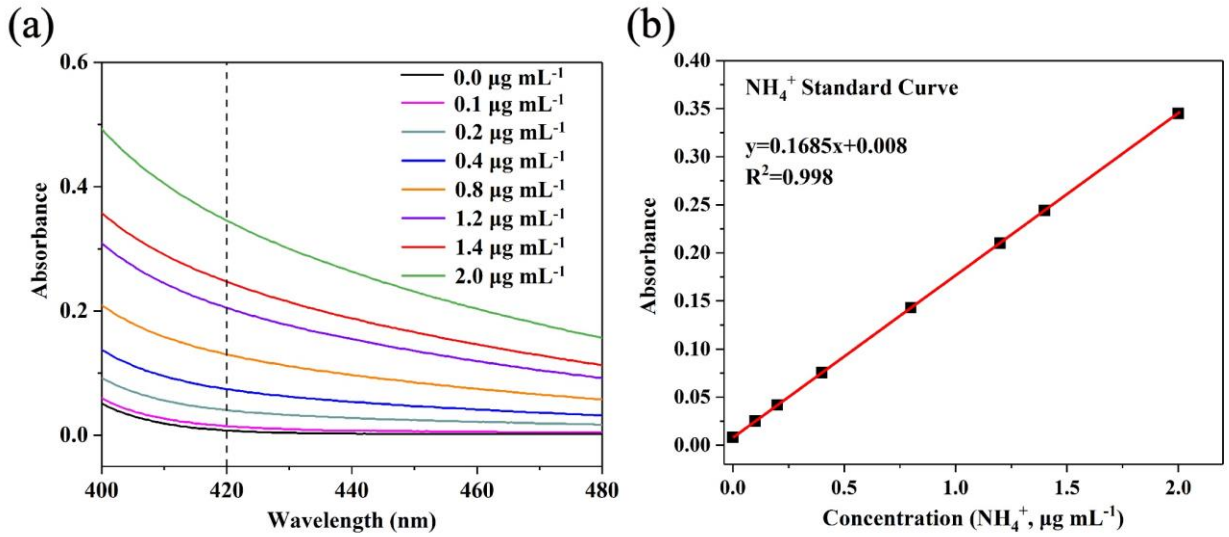

Fig. S8. (a) UV-Vis absorption curves of Nessler's reagent assays kept with different concentrations of NH_4^+ ions. (b) A calibration curve used to estimate the concentrations of NH_4^+ ions.

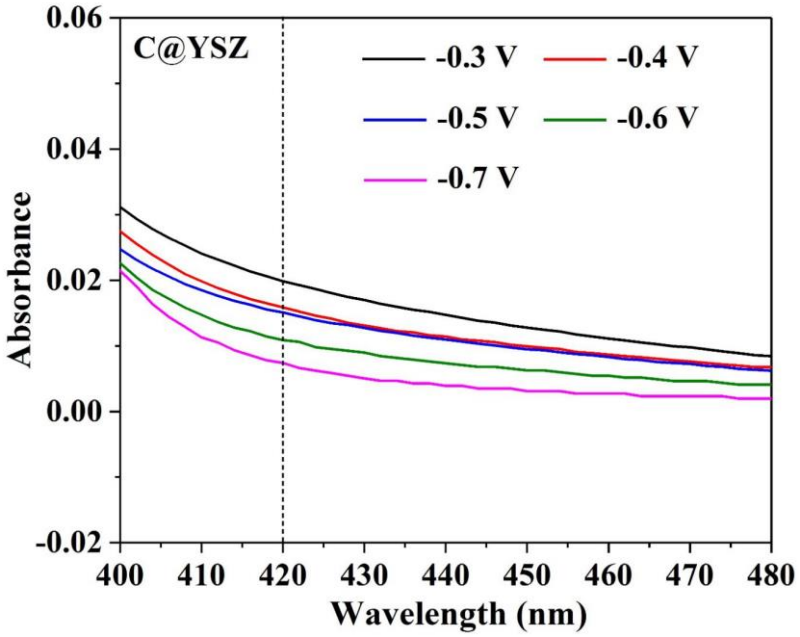

Fig. S9. UV-Vis absorption curves of the electrolyte after tests of C@YSZ at different potentials.

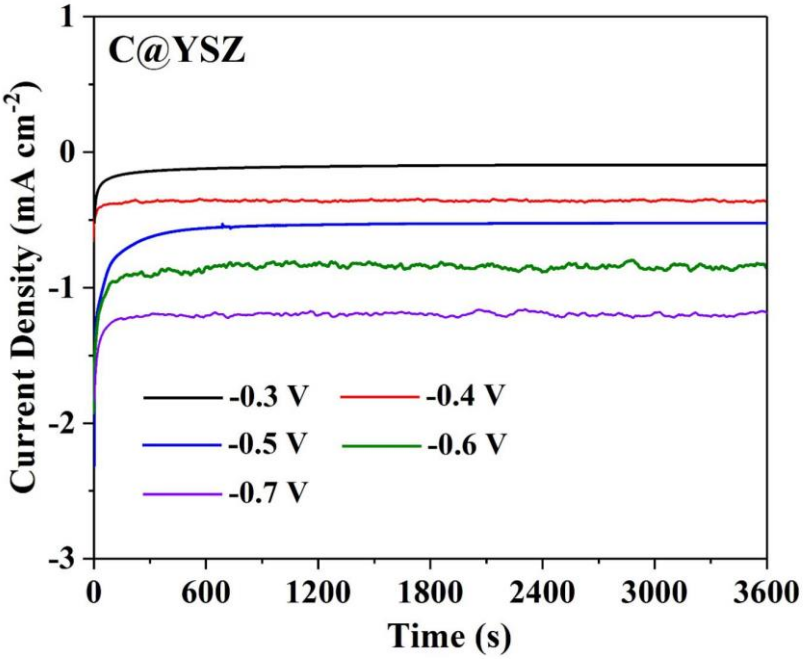

Fig. S10. Time-dependent current density curve for C@YSZ at different potentials.

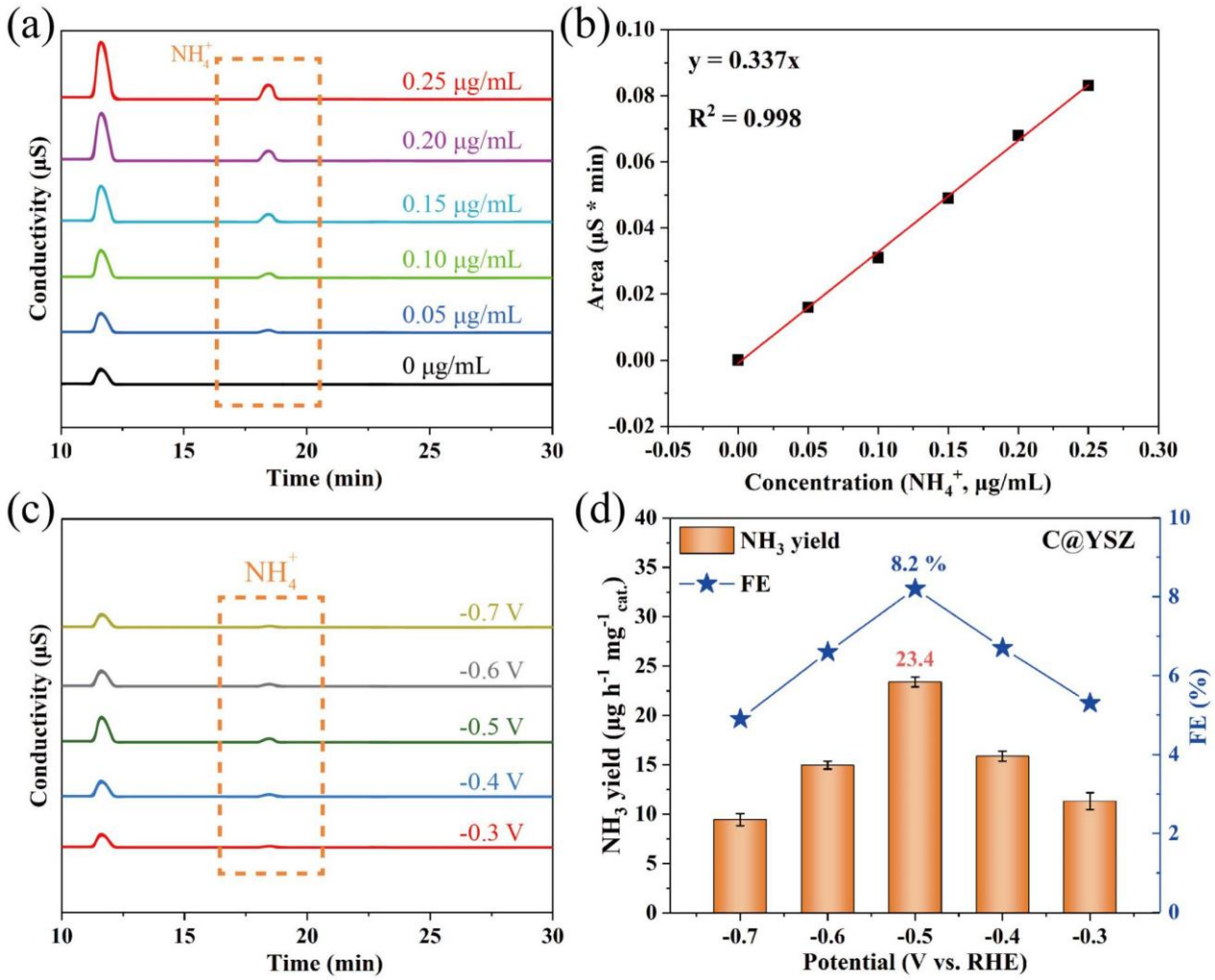

Fig. S11. (a) Ion chromatograms of NH_4^+ with different concentrations in 0.1 M Na_2SO_4 and (b) corresponding standard curve. (c) Ion chromatogram data for the electrolytes at a series of potentials after electrolysis for 1 h. (d) NH_3 yields and FEs for C@YSZ at corresponding potentials calculated by ion chromatography.

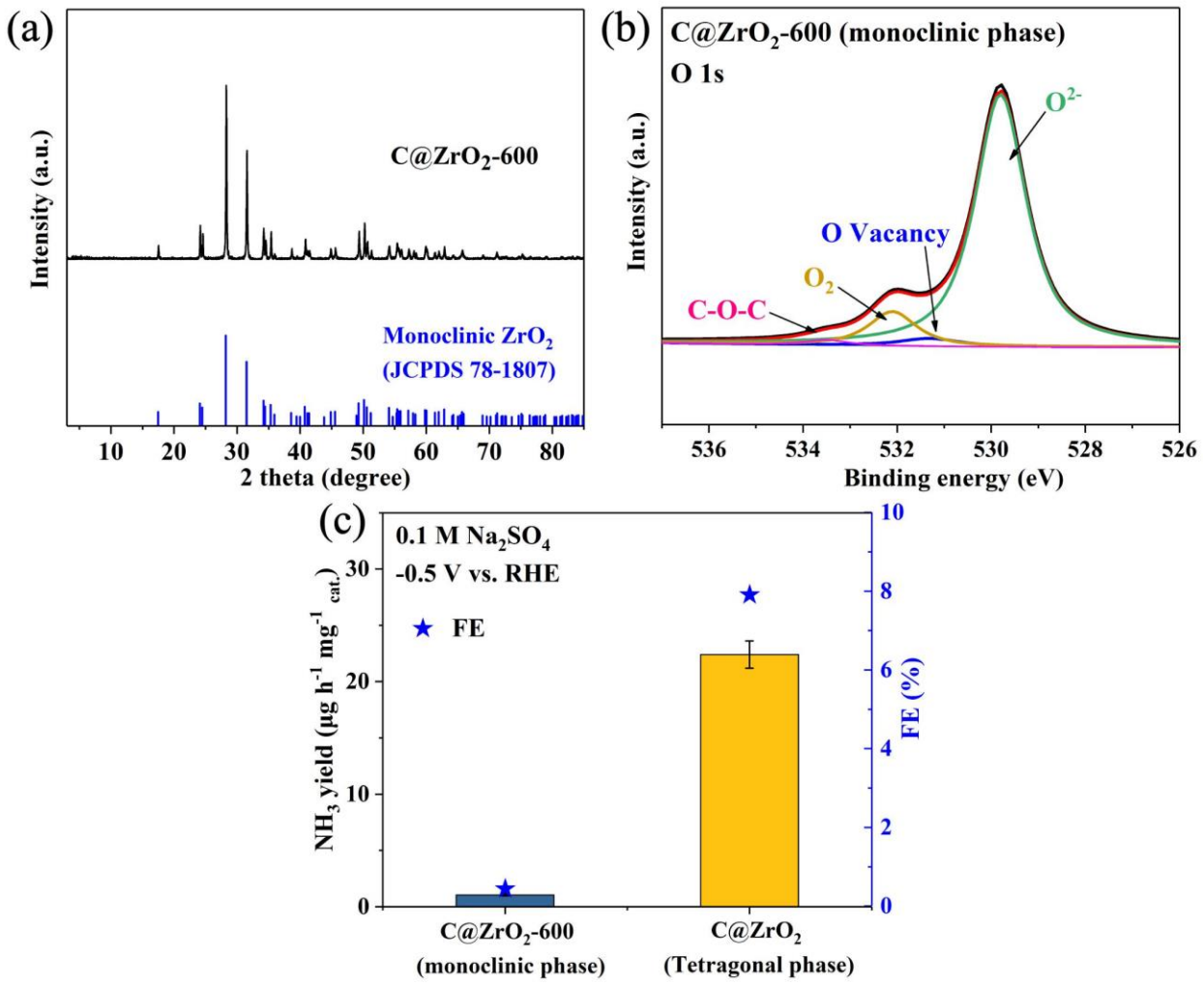

Fig. S12. (a) XRD pattern, (b) O 1s XPS pattern of monoclinic C@ZrO_2-600. (c) NRR performance of C@ZrO_2-600 and C@ZrO_2.

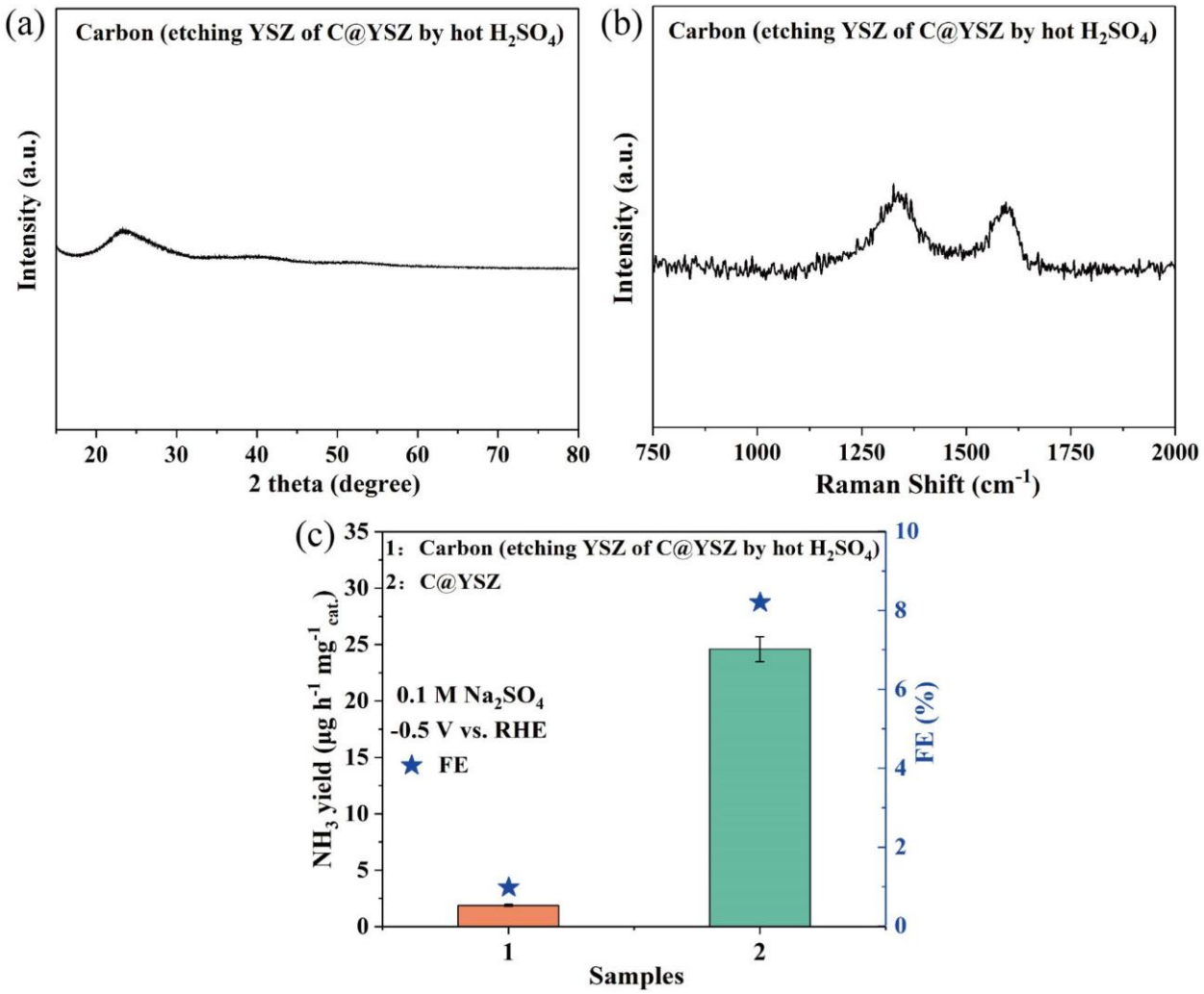

Fig. S13. (a) XRD pattern, (b) Raman pattern of carbon (etching YSZ of C@YSZ by hot H_2SO_4). (c) NRR performance of carbon (etching YSZ C@YSZ by hot H_2SO_4) and C@YSZ.

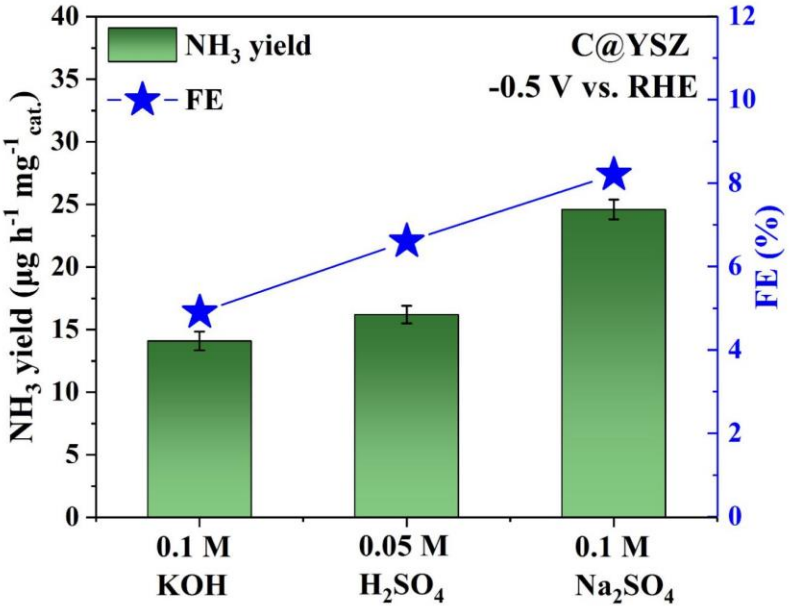

Fig. S14. NRR performance of C@YSZ in different electrolytes at -0.5 V.

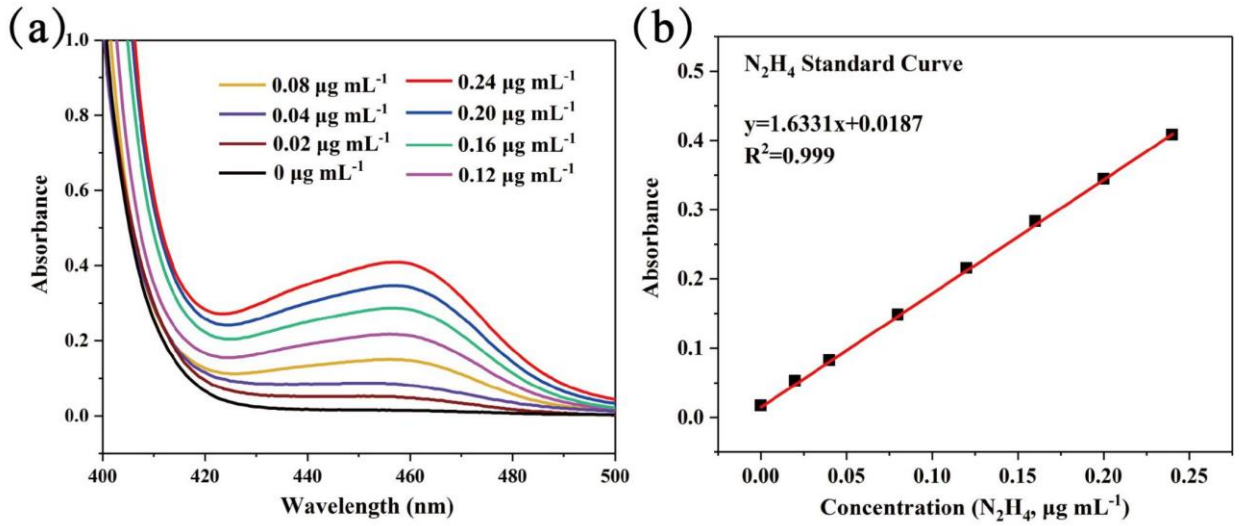

Fig. S15. (a) UV-Vis curves of various concentrations of N_2H_4 stained with p-$C_9H_{11}NO$ indicator. (b) A calibration curve used to estimate the concentrations of N_2H_4.

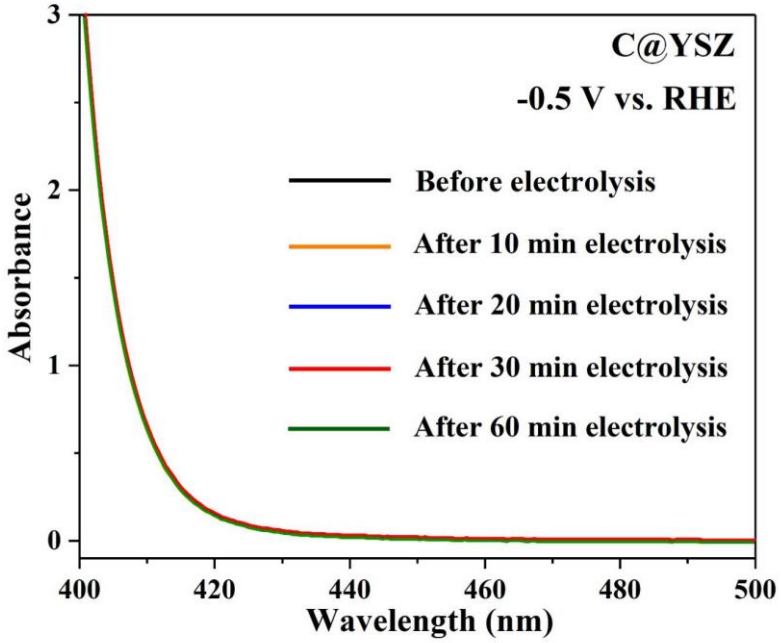

Fig. S16. UV-Vis absorption spectra of the electrolytes stained with p-$C_9H_{11}NO$ indicator after NRR electrolysis at different time.

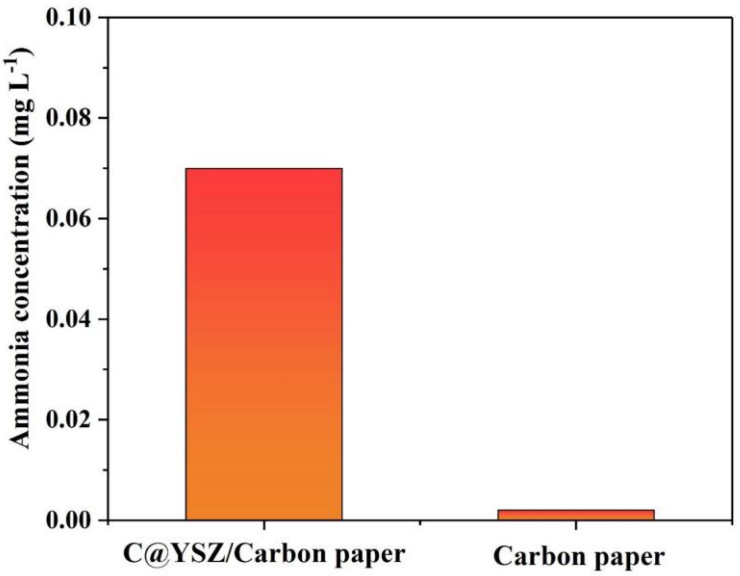

Fig. S17. Ammonia concentration of C@YSZ/CP and CP after 1 h electrolysis at a potential of -0.5 V under ambient conditions.

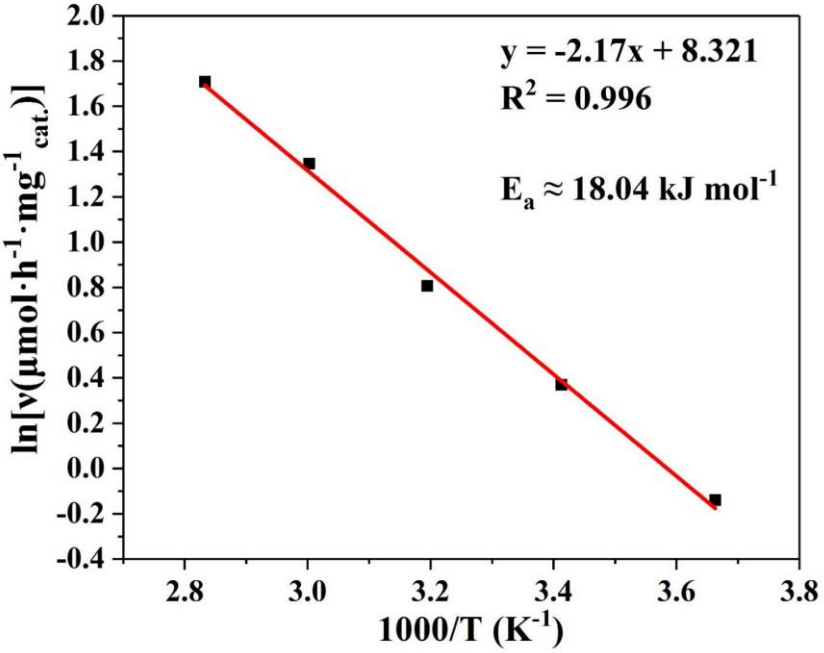

Fig. S18. Arrhenius plot of the NRR rate over C@YSZ catalyst at the temperature from 273 to 353 K.

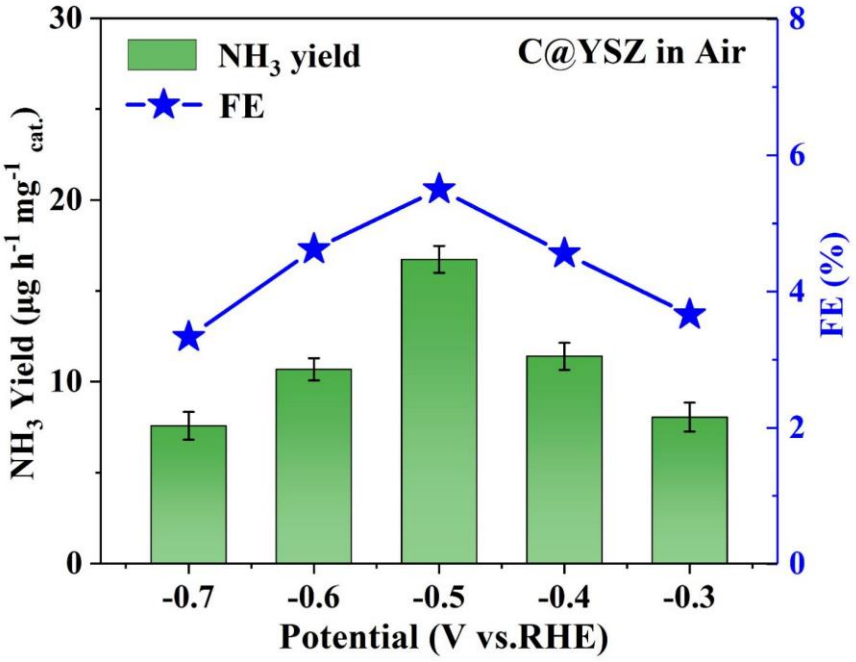

Fig. S19. NH_3 yields and FE for C@YSZ at different potentials in Air.

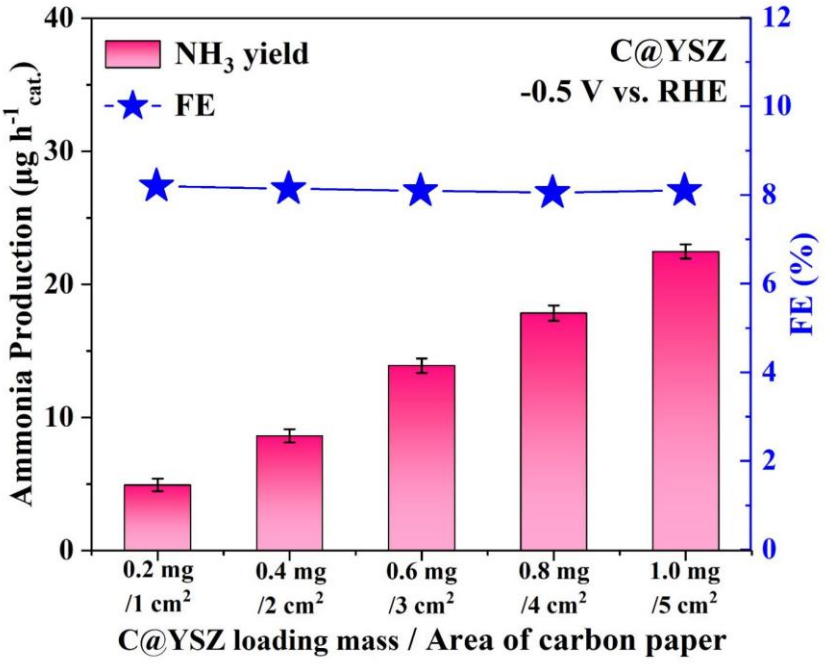

Fig. S20. NH_3 production and FE against the size of working electrode.

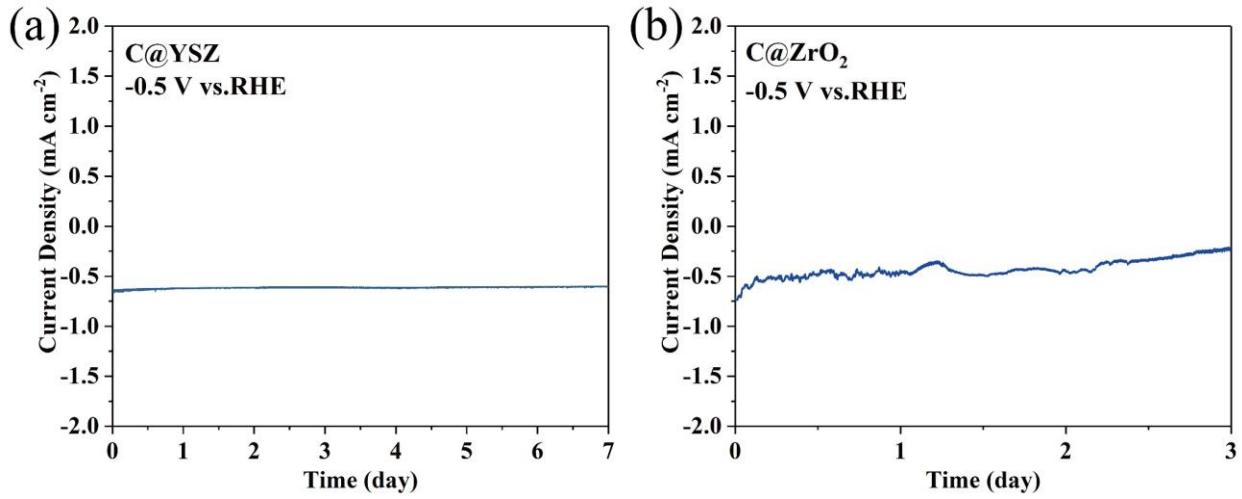

Fig. S21. (a) Time-dependent current density curve for C@YSZ in 7 days. (b) Time-dependent current density curve for C@ZrO_2 in 3 days.

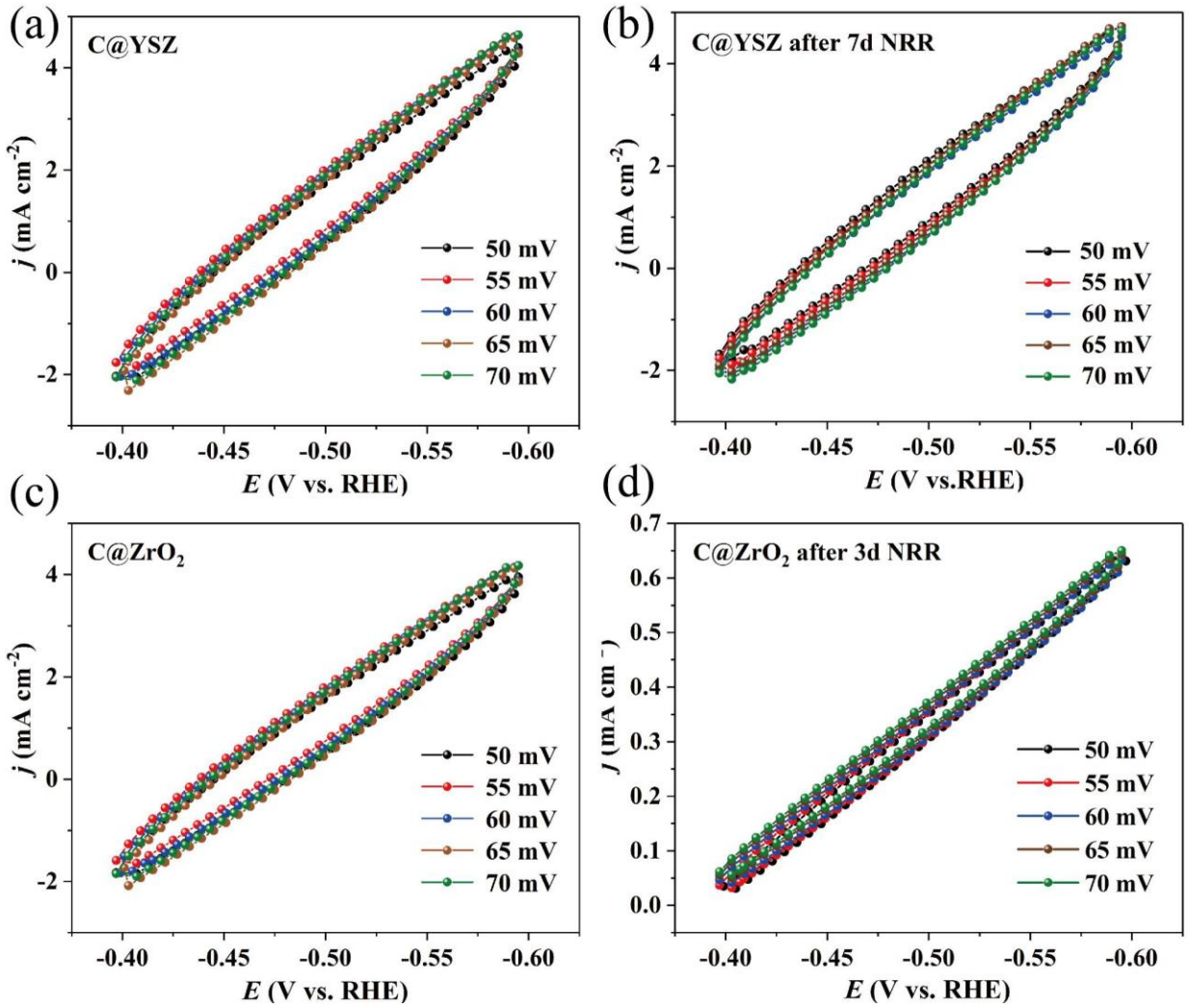

Fig. S22. The electrochemically active surface area characterization of (a) C@YSZ, (b) C@YSZ after 7 days NRR, (c) C@ZrO_2 and (d) C@ZrO_2 after 3 days NRR. All cyclic voltammetry curves were measured in non-faradaic capacitance current range at a scan rate of 50, 55, 60, 65 and 70 mV s^{-1}.

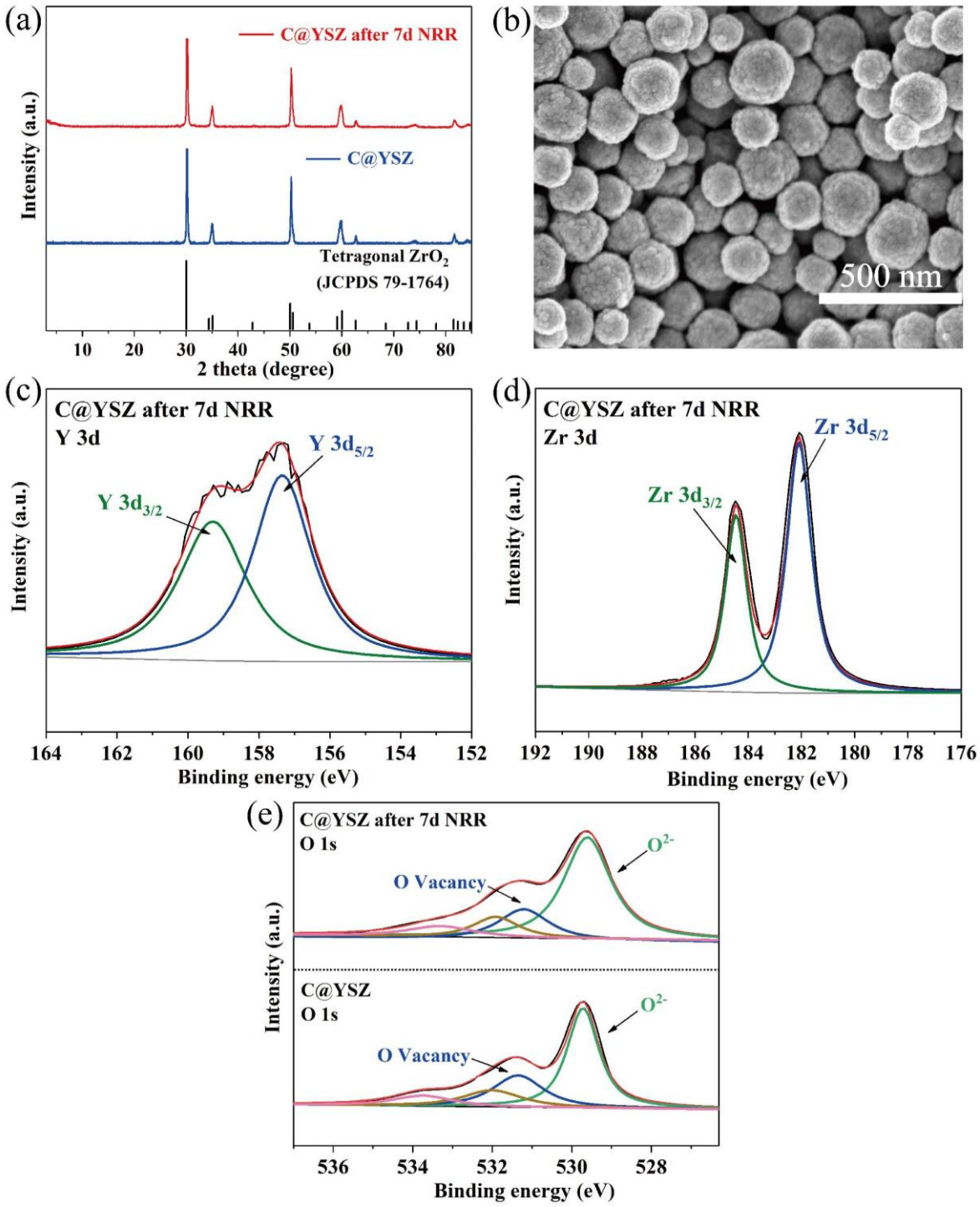

Fig. S23. (a) XRD pattern, (b) SEM image, (c) XPS Y 3d spectra, (d) XPS Zr 3d spectra and (e) XPS O 1s spectra of C@YSZ after 7 days NRR.

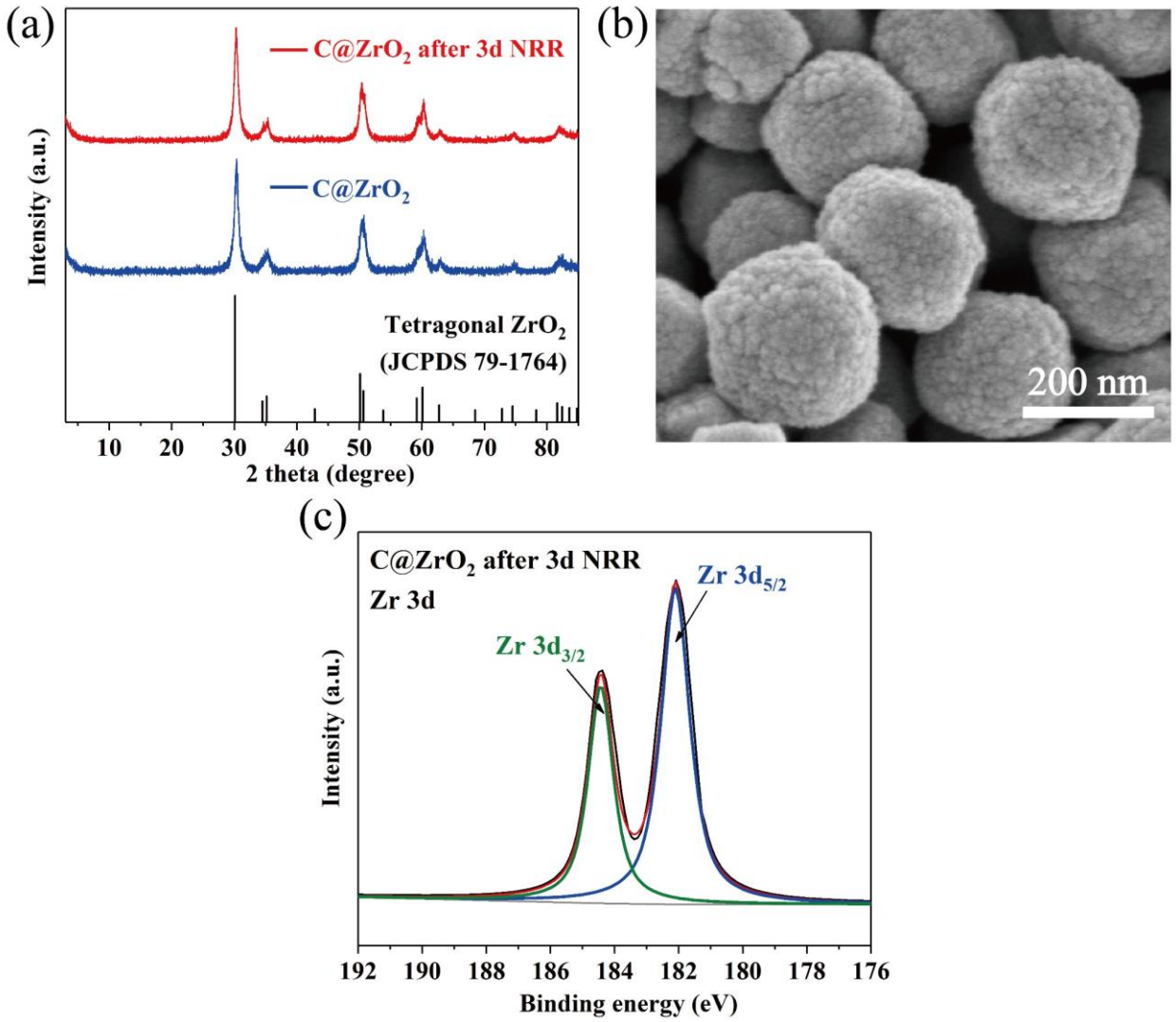

Fig. S24. (a) XRD pattern, (b) SEM image, (c) XPS Zr 3d spectra of C@ZrO_2 after 3 days NRR.

Table S1. Comparison of the electrocatalytic activity of C@YSZ to produce NH_3 through NRR with respect to the performances of other newly reported NRR electrocatalysts.

Catalyst	Electrolyte	NH_3 yield ($\mu g\ h^{-1}\ mg^{-1}$)	FE (%)	Stability	Reference
C@YSZ	**0.1 M Na_2SO_4**	**24.6**	**8.2**	**7 days**	**This work**
Cr-doped CeO_2	0.1 M Na_2SO_4	16.82	3.84	24 h	*Inorg. Chem.* 2019, **58**, 5423-5427
Bi_2MoO_6	0.1 M HCl	20.46	8.17	24 h	*ACS Sustain. Chem. Eng.* 2019, **7**, 12692-12696
Co_3O_4@NC	0.05M H_2SO_4	42.58	8.49	24 h	*ACS Appl. Mater. Inter.* 2019, **11**, 26891-26897
C@NiO@Ni	0.1 M KOH	43.15	10.9	72 h	*Sustain. Energ. Fuels.* 2020, **4**, 164-170
Pd/C	0.1 M PBS	4.5	8.2	15 h	*Nat. Commun.* 2018, **9**, 1795
N-doped porous carbon	0.05 M H_2SO_4	23.8	1.42	20 h	*ACS Catal.* 2018, **8**, 1186-1191
MoO_3	0.1 M HCl	29.43	1.9	24 h	*J. Mater. Chem. A* 2018, **6**, 12974-12977
Nb_2O_5 nanofiber	0.1 M HCl	43. 5	9.26	27 h	*Nano Energy* 2018, **52**, 264-270
hollow Cr_2O_3 microspheres	0.1 M Na_2SO_4	25. 3	6.78	24 h	*ACS Catal.* 2018, **8**, 8540-8544
Mn_3O_4	0.1 M Na_2SO_4	11. 6	3.0	24 h	*Small* 2018, **14**, e1803111
MoS_2 Nanoflower	0.1 M Na_2SO_4	29. 3	8.34	26 h	*Adv. Energy. Mater.* 2018, **8**, 1801357
b-FeOOH nanorods	0.5 M $LiClO_4$	23. 3	6.7	24 h	*Chem. Commun.* 2018, **54**, 11332-11335
TiO_2–rGO	0.1 M Na_2SO_4	15. 1	3.3	24 h	*J. Mater. Chem. A* 2018, **6**, 17303-17306
B_4C	0.1 M HCl	26. 6	16.0	30 h	*Nat. Commun.* 2018, **9**, 3485
$Bi_4V_2O_{11}/CeO_2$	0.1 M HCl	23.21	10.16	8 h	*Angew. Chem., Int. Ed.* 2018, **57**, 6073-6076.

$TiO_2/Ti_3C_2T_x$	0.1 M HCl	26.32	8.42	24 h	*Inorg. Chem.* 2019, **58**, 5414-5418
NiO/Graphene	0.1 M Na_2SO_4	18.6	7.8	32 h	*ACS Appl. Energy Mater.* 2019, **2**, 2288-2295
Fe_{SA}–N–C	0.001 M H_2SO_4	7.48	56.55	30 h	*Nat. Commun*. 2019, **10**, 341
$K_2Ti_4O_9$	0.1 M KOH	22.88	5.87	24 h	*Chem. Commun.* 2019, **55**, 7546-7549
$LiMn_2O_4$	0.1 M HCl	15.83	7.44	24 h	*Inorg. Chem.* 2019, **58**, 9597-9601
CeO_2-rGO	0.1 M Na_2SO_4	16.98	4.78	24 h	*Chem. Commun.* 2019, **55**, 10717-10720
$MnO_2/Ti_3C_2T_x$	0.1 M HCl	34.12	11.39	24 h	*J. Mater. Chem. A.* 2019, **7**, 18823-18827
$Ti_3C_2T_x$	0.1 M HCl	20.4	9.3	23 h	*J. Mater. Chem. A.* 2018, **6**, 24031-24035
SnO_2/RGO	0.1 M Na_2SO_4	25.6	7.1	10 h	*ACS Appl. Mater. Inter.* 2019, **11**, 31806-31815
Sn/SnS_2	0.1 M HCl	23.8	3.4	10 h	*Small*. 2019, **15**, 1902535
Ta_2O_5	0.1 M HCl	15.9	8.9	24 h	*ACS Sustain. Chem. Eng.* 2019, **7**, 9622-9628
Y_2O_3	0.1 M Na_2SO_4	64.87	2.53	20 h	*Ind. Eng. Chem. Res.* 2018, **57**, 16622−16627
ZnO/RGO	0.1 M Na_2SO_4	17.7	6.4	10 h	*Chem. Eur. J.* 2019, **15**, 1902535
$TiO_2/Ti_3C_2T_x$	0.1 M HCl	32.17	16.07	50 h	*Adv. Energy Mater.* 2019, **9**, 1803406
Cr_3C_2@CNF	0.1 M HCl	23.9	8.6	24 h	*ACS Appl. Mater. Inter.* 2019, **11**, 35764-35769
$CoFe_2O_4$	0.1 M Na_2SO_4	0.151	6.2	8 h	*Chem. Commun.* 2019, **55**, 12184-12187

Fe_3C@C	0.05 M H_2SO_4	8.53	9.15	12 h	*ACS Appl. Mater. Inter.* 2019, **11**, 40062−40068
$NbSe_2$	0.1 M Na_2SO_4	89.5	13.9	60 h	*Journal of Catalysis* 2020, **381**, 78-83
N-C@NiO/GP	0.1 M HCl	14.02	30.43	20 h	*ACS Sustain. Chem. Eng.* 2019, **7**, 18874−18883
WO_3	0.1 M HCl	17.28	7.0	24 h	*Nanoscale* 2019, **11**, 19274-19277
TiC/C	0.1 M HCl	14.1	5.8	24 h	*J. Mater. Chem. A* 2019, **7**, 19657-19661
LaF_3	0.5 M $LiClO_4$	55.9	16.0	24 h	*J. Mater. Chem. A* 2019, **7**, 17761-17765
$La_2Ti_2O_7$	0.1 M HCl	21.15	4.55	24 h	*Chem. Commun.* 2019, **55**, 6401-6404